A Properly Designed Extended Kalman Filtering Approach for Robot Localization by Sensors with Different Degree of...

Conference Paper · August 2004

DOI: 10.13140/2.1.3322.1448

CITATIONS
3

READS
49

4 authors, including:

Leopoldo Jetto
Università Politecnica delle Marche
130 PUBLICATIONS **1,013** CITATIONS
SEE PROFILE

S. Longhi
Università Politecnica delle Marche
382 PUBLICATIONS **3,335** CITATIONS
SEE PROFILE

Andrea Monteriù
Università Politecnica delle Marche
99 PUBLICATIONS **428** CITATIONS
SEE PROFILE

A Properly Designed Extended Kalman Filtering Approach for Robot Localization by Sensors with Different Degree of Accuracy

G. Ippoliti, L. Jetto, S. Longhi and A. Monteriù
Università Politecnica delle Marche,
Dipartimento di Ingegneria Informatica,
Gestionale e dell'Automazione,
Via Brecce Bianche, 60131 Ancona, Italy.
Tel.: +39 071 220 4451, Fax: +39 071 220 4474,
Email: g.ippoliti@diiga.univpm.it
{l.jetto, sauro.longhi, a.monteriu}@univpm.it

***Abstract*— A basic requirement for an autonomous mobile robot is to localize itself with respect to a given coordinate system. In this regard two different operating conditions exist: structured and unstructured environment. The relative methods and algorithms are strongly influenced by the *a priori* knowledge on the environment where the robot operates. If the environment is only partially known the localization algorithm needs a preliminary definition of a suitable environment map. In this paper the localization problem is formulated in a stochastic setting and an Extended Kalman Filtering (EKF) approach is proposed for the integration of odometric, gyroscope and laser scanner measures. As gyroscopic measures are much more reliable than the other ones, the localization algorithm gives rise to a nearly singular EKF. This problem is dealt with defining a lower order non singular EKF.**

I. INTRODUCTION

Two different kinds of mobile robot localization exist: relative and absolute. The first one is based on the data provided by sensors measuring the dynamics of variables internal to the vehicle; absolute localization requires sensors measuring some parameters of the environment where the robot is operating. The actual trend is to exploit the complementary nature of these two kinds of sensorial information to improve the precision of the localization procedure (see e.g. [1]–[6]) at expense of an increased cost and computational complexity.

The aim is to improve the mobile robot autonomy by enhancing its capability of localization with respect to the surrounding environment. In this framework the research interests have been focused on multi-sensor systems because of the limitations inherent any single sensory device, that can only supply a partial information on the environment, thus limiting the ability of the robot to localize itself. The methods and algorithms proposed in the literature for an efficient integration of multiple-sensor information differ according to the *a priori* information on the environment, which may be almost known and static, or almost unknown and dynamic.

If the environment is only partially known the localization algorithm needs a preliminary definition of a suitable environment map.

Recently, the Simultaneous Localization and Map Building problem (SLAM problem) has been deeply investigated for increasing the autonomy of navigation of mobile robots (see e.g. [7]–[23]). The idea is to develop a localization algorithm that can build a map of the environment while simultaneously using the same map to localize the mobile robot. This approach promises to allow these vehicles to really operate autonomously for long period of time in unknown environments.

The purpose of this paper is to propose and to experimentally evaluate a localization algorithm based on a measure apparatus composed of a set of sensors of a different nature and characterized by a highly different degree of accuracy. The sensor equipment includes odometric, gyroscopic and laser measures.

In particular, the interest of this paper focuses on the emerging area of assistive technologies where powered wheelchairs can be used to strengthen the residual abilities of users with motor disabilities [24]–[26].

The proposed algorithm results in a computationally efficient solution of the localization problem and may really represent a first basic step towards the proper design of a navigation system aimed at enhancing the efficiency and the security of commercial powered wheelchairs.

The main technical novelties of this paper are: i) both the information carried by the kinematic model of the robot and that carried by the dynamic equations of the odometry are exploited. The first kind of information is inglobed in the dynamical equation of the state-space model of the vehicle, the second one is properly inglobed in a measure equation through the definition of an extended state; ii) the nearly singular filtering problem arising from the very high accuracy of a measure has been explicitly taken into account.

The experimental tests, performed on the TGR Explorer

powered wheelchair [27] in an indoor environment, show a significant improvement of the performance of the vehicle localization module with respect to previously tested EKF integrating odometric, gyroscopic and sonar measures [2], [6].

II. The sensor equipment

A. Odometric measures

Consider an unicycle-like mobile robot with two driving wheels, mounted on the left and right sides of the robot, with their common axis passing through the center of the robot (see Figure 1). Localization of this mobile robot

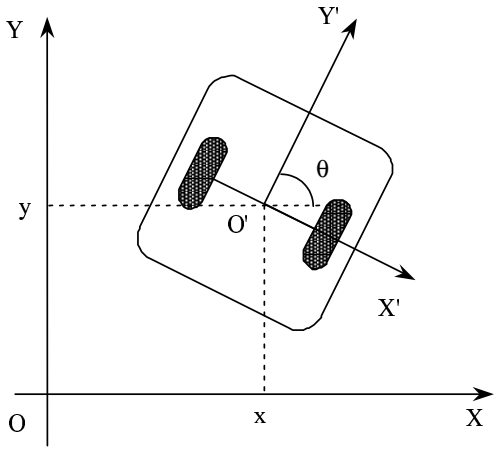

Fig. 1. Scheme of the unicycle mobile robot.

in a two-dimensional space requires the knowledge of coordinates x and y of the midpoint between the two driving wheels and of the angle θ between the main axis of the robot and the X-direction. The kinematic model of the unicycle robot is described by the following equations:

$$\dot{x}(t) = \nu(t)cos\theta(t), \quad (1)$$
$$\dot{y}(t) = \nu(t)sin\theta(t), \quad (2)$$
$$\dot{\theta}(t) = \omega(t), \quad (3)$$

where $\nu(t)$ and $\omega(t)$ are, respectively, the displacement and angular velocities of the robot, and are expressed by:

$$\nu(t) = \frac{\omega_r(t) + \omega_l(t)}{2} r, \quad (4)$$
$$\omega(t) = \frac{\omega_r(t) - \omega_l(t)}{d} r, \quad (5)$$

where $\omega_r(t)$ and $\omega_l(t)$ are the angular velocities of the right and left wheels, respectively, r is the wheel radius and d is the distance between the wheels.

Assuming constant $\omega_r(t)$ and $\omega_l(t)$ over a sufficiently small sampling period $\Delta t_k := t_{k+1} - t_k$, the position and orientation of the robot at time instant t_{k+1} can be expressed as [28]:

$$x(t_{k+1}) = x(t_k) + \bar{\nu}(t_k)\Delta t_k \frac{sin\frac{\bar{\omega}(t_k)\Delta t_k}{2}}{\frac{\bar{\omega}(t_k)\Delta t_k}{2}} \times cos(\theta(t_k) + \frac{\bar{\omega}(t_k)\Delta t_k}{2}), \quad (6)$$

$$y(t_{k+1}) = y(t_k) + \bar{\nu}(t_k)\Delta t_k \frac{sin\frac{\bar{\omega}(t_k)\Delta t_k}{2}}{\frac{\bar{\omega}(t_k)\Delta t_k}{2}} \times sin(\theta(t_k) + \frac{\bar{\omega}(t_k)\Delta t_k}{2}), \quad (7)$$

$$\theta(t_{k+1}) = \theta(t_k) + \bar{\omega}(t_k)\Delta t_k. \quad (8)$$

where $\bar{\nu}(t_k)\Delta t_k$ and $\bar{\omega}(t_k)\Delta t_k$ are:

$$\bar{\nu}(t_k)\Delta t_k = \frac{\Delta q_r(t_k) + \Delta q_l(t_k)}{2} r, \quad (9)$$
$$\bar{\omega}(t_k)\Delta t_k = \frac{\Delta q_r(t_k) - \Delta q_l(t_k)}{d} r. \quad (10)$$

The terms $\Delta q_r(t_k)$ and $\Delta q_l(t_k)$ are the incremental distances covered on the interval Δt_k by the right and left wheels of the robot respectively. Denote by $y_r(t_k)$ and $y_l(t_k)$ the measures of $\Delta q_r(t_k)$ and $\Delta q_l(t_k)$ respectively, provided by the encoders attached to wheels, one has

$$y_r(t_k) = \Delta q_r(t_k) + s_r(t_k), \quad (11)$$
$$y_l(t_k) = \Delta q_l(t_k) + s_l(t_k), \quad (12)$$

where $s_r(\cdot)$, $s_l(\cdot)$ are the measurement errors, which are modelled as independent, zero mean, gaussian white sequences $(s_r(\cdot) \sim N(0, \sigma_r^2)$, $(s_l(\cdot) \sim N(0, \sigma_l^2)$ [28]. It follows that the really available values $y_\nu(t_k)$ and $y_\omega(t_k)$ of $\bar{\nu}(t_k)\Delta t_k$ and $\bar{\omega}(t_k)\Delta t_k$ respectively are given by

$$y_\nu(t_k) = \frac{y_r(t_k) + y_l(t_k)}{2} r = \bar{\nu}(t_k)\Delta t_k + n_\nu(t_k), \quad (13)$$

$$y_\omega(t_k) = \frac{y_r(t_k) - y_l(t_k)}{d} r = \bar{\omega}(t_k)\Delta t_k + n_\omega(t_k), \quad (14)$$

where $n_\nu(\cdot)$ and $n_\omega(\cdot)$ are independent, zero mean, gaussian white sequences $(n_\nu(\cdot) \sim N(0, \sigma_\nu^2)$, $(n_\omega(\cdot) \sim N(0, \sigma_\omega^2)$, where, by (9) and (10), $\sigma_\nu^2 = (\sigma_r^2 + \sigma_l^2)r^2/4$ and $\sigma_\omega^2 = (\sigma_r^2 + \sigma_l^2)r^2/d^2$.

B. Fiber optic gyroscope measures

The operative principle of a Fiber Optic Gyroscope (FOG) is based on the Sagnac effect. The FOG is made of a fiber optic loop, fiber optic components, a photodetector and a semiconductor laser. The phase difference of the two light beams traveling in opposite directions around the fiber optic loop is proportional to the rate of rotation of the fiber optic loop. The rate information is internally integrated to provide the absolute measurements of orientation. A FOG does not require frequent maintenance and have a longer lifetime of the conventional mechanical gyroscopes. In a FOG the drift is also low.

A complete analysis of the accuracy and performance of this internal sensor has been developed in [29]–[32]. This internal sensor represents a simple low cost solution for producing accurate pose estimation of a mobile robot. The FOG readings are denoted by $\theta_g(\cdot) = \theta_g^r(\cdot) + n_\theta(\cdot)$, where $\theta_g^r(\cdot)$ is the true value and $n_\theta(\cdot)$ is an independent, zero mean, gaussian white sequence ($n_\theta(\cdot) \sim N(0, \sigma_\theta^2)$).

C. Laser scanner measures

The distance readings by the Laser Measurement System (LMS) are related to the in-door environment model and to the configuration of the mobile robot.

Denote with l the distance between the center of the laser scanner and the origin O' of the coordinate system (O', X', Y') fixed to the mobile robot, as reported in Figure 2. At the sampling time t_k, the position x_s, y_s

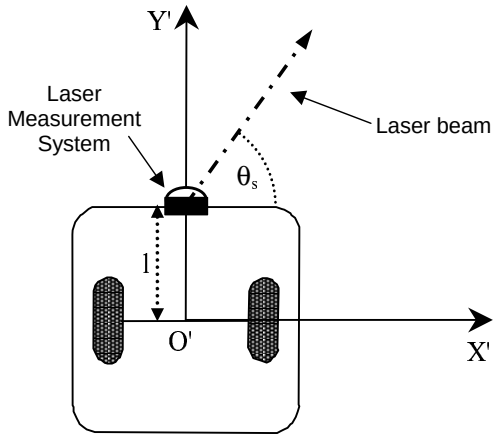

Fig. 2. Laser scanner displacement.

and orientation θ_s of the center of the laser scanner, referred to the inertial coordinate system (O, X, Y), have the following form:

$$x_s(t_k) = x(t_k) + l\,cos\theta(t_k), \quad (15)$$

$$y_s(t_k) = y(t_k) + l\,sin\theta(t_k), \quad (16)$$

$$\theta_s(t_k) = \theta(t_k). \quad (17)$$

The walls and the obstacles in an in-door environment are represented by a proper set of planes orthogonal to the plane XY of the inertial coordinate system. Each plane $P^j, j = 1, 2, \ldots, n_p$, (where n_p is the number of planes which describe the in-door environment), is represented by the triplet P_r^j, P_n^j and P_ν^j, where P_r^j is the normal distance of the plane from the origin O, P_n^j is the angle between the normal line to the plane and the X-direction and P_ν^j is a binary variable, $P_\nu^j \in \{-1,\ 1\}$, which defines the face of the plane reflecting the laser beam. In such a notation, the expectation of the $i-th$ ($i = 1, 2, \cdots, n_s$) laser reading $d_i^j(t_k)$, relative to the present distance of the center of the laser scanner from the plane P^j, has the following expression (see Figure 3):

$$d_i^j(t_k) = \frac{P_\nu^j(P_r^j - x_s(t_k)cosP_n^j - y_s(t_k)sinP_n^j)}{cos\theta_d^j}, \quad (18)$$

where

$$\theta_d^j = P_n^j - \theta^* \quad (19)$$

with $\theta^* \in [\theta_0,\ \theta_1]$ given by (see Figure 4):

$$\theta^* = \theta + \theta_r - \frac{\pi}{2}. \quad (20)$$

The vector composed of geometric parameters P_r^j, P_n^j, P_ν^j, $j = 1, 2, \ldots, n_p$, is denoted by Π.

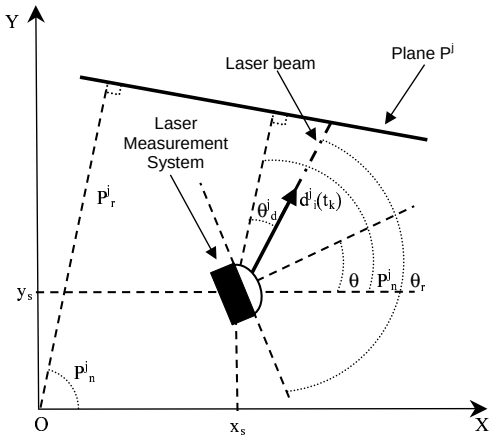

Fig. 3. Laser scanner measure.

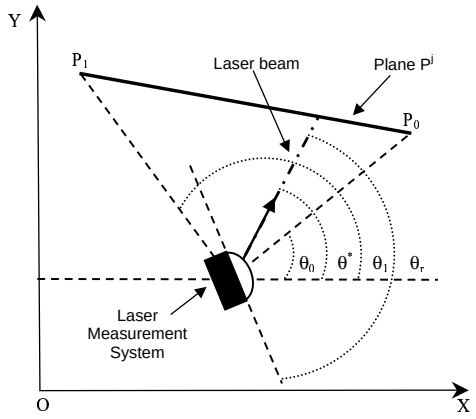

Fig. 4. Laser scanner field of view for plane P^j.

III. Estimation of robot location

The algorithm operates in a stochastic framework and is based on the ascertainment that the angular measure $\theta_g(t_k)$ provided by the FOG is much reliable than the angular measure $y_\omega(t_k)$ obtainable by encoders. In [28], it has been shown that the incremental errors on the encoder readings especially affect the estimate of the orientation and reduce their applicability to short trajectories.

A state-space approach is adopted with the purpose of defining a more general method merging the information carried by the vehicle model with that provided by the sensor equipment. The estimation algorithm is an Extended Kalman Filter (EKF) defined on the basis of a state equation derived from (1)–(3) and of a measure equation containing the incremental measures of the encoders $y_\nu(t_k)$, the angular measure of the gyroscope $\theta_g(t_k)$ and the distance measures provided by the laser scanner from the P^j plane, $1 \le j \le n_p$.

Denote with $X(t) := [x(t),\, y(t),\, \theta(t)]^T$ the true robot state and with $U(t) := [\nu(t),\, \omega(t)]^T$ the robot control input. For future manipulations it is convenient to partition $X(t)$ as $X(t) = [X_1(t)^T,\, \theta(t)]^T$, with $X_1(t) = [x(t),\, y(t)]^T$. The kinematic model of the robot can be written in the compact form of the following stochastic differential equation

$$dX(t) = F(X(t), U(t))dt + d\eta(t), \tag{21}$$

where $F(X(t), U(t))$ represents the set of equations (1)–(3) and $\eta(t)$ is a Wiener process such that $E(d\eta(t)d\eta(t)^T) = Qdt$. Its weak mean square derivative $d\eta(t)/dt$ is a white noise process $\sim N(0, Q)$ representing the model inaccuracies (parameter uncertainties, slippage, dragging). It is assumed that $Q = \sigma_\eta^2 I_3$. The diagonal form of Q understands the hypothesis that model (21) describes the true dynamics of the three state variables with nearly the same degree of approximation and with independent errors.

Let $\Delta t_k = T$ be the constant sampling period and denote t_{k+1} by $(k+1)T$, assume $U(t) = U(kT) := U(k)$, for $t \in [kT,\, (k+1)T)$, and denote by $X(k)$ and by $\hat{X}(k,k)$ the current state and its filtered estimate respectively, at time instant $t = kT$. Linearization of (21) about $U(k-1)$ and $\hat{X}(k,k)$ and subsequent discretization with period T results in the following equation

$$X(k+1) = A_d(k)X(k,k) + L(k)U(k) + D(k) + W(k). \tag{22}$$

Partitioning vectors and matrices on the right hand side of equation (22) accordingly to the partition of the state vector one has:

$$A_d(k) = \exp(A(k)T) = \begin{bmatrix} A_{1,1_d}(k) & A_{1,2_d}(k) \\ A_{2,1_d}(k) & A_{2,2_d}(k) \end{bmatrix}, \tag{23}$$

$$L(k) = \begin{bmatrix} L_1(k) \\ L_2(k) \end{bmatrix}, \quad D(k) = \begin{bmatrix} D_1(k) \\ D_2(k) \end{bmatrix}, \tag{24}$$

$$\begin{aligned} A(k) &:= \left[\frac{\partial F(X(t), U(t))}{\partial X(t)}\right]_{\substack{X(t)=\hat{X}(k,k) \\ U(t-1)=U(k-1)}} \\ &= \begin{bmatrix} 0 & 0 & -\nu(k-1)\sin\hat{\theta}(k,k) \\ 0 & 0 & \nu(k-1)\cos\hat{\theta}(k,k) \\ 0 & 0 & 0 \end{bmatrix}, \end{aligned} \tag{25}$$

$$A_{1,1_d}(k) = \begin{bmatrix} 1 & 0 \\ 0 & 1 \end{bmatrix} := I_2, \tag{26}$$

$$A_{1,2_d}(k) = \begin{bmatrix} -\nu(k-1)\sin\hat{\theta}(k,k)T \\ \nu(k-1)\cos\hat{\theta}(k,k)T \end{bmatrix}, \tag{27}$$

$$A_{2,1_d}(k) = [0,\, 0], \quad A_{2,2_d}(k) = 1, \tag{28}$$

$$L_1(k) = \begin{bmatrix} Tcos\hat{\theta}(k,k) & -0.5\nu(k-1)T^2 sin\hat{\theta}(k,k) \\ Tsin\hat{\theta}(k,k) & 0.5\nu(k-1)T^2 cos\hat{\theta}(k,k) \end{bmatrix}, \tag{29}$$

$$L_2(k) = [0,\, T], \tag{30}$$

$$D_1(k) = \begin{bmatrix} T\nu(k-1)\hat{\theta}(k,k)\sin\hat{\theta}(k,k) \\ -T\nu(k-1)\hat{\theta}(k,k)\cos\hat{\theta}(k,k) \end{bmatrix},\ D_2(k) = 0, \tag{31}$$

$$\begin{aligned} W(k) &:= \int_{kT}^{(k+1)T} \exp(A(k)[(k+1)T - \tau])\eta(\tau)d\tau \\ &= \begin{bmatrix} W_1(k) \\ W_2(k) \end{bmatrix}, \end{aligned} \tag{32}$$

with $W_1(k) \in \mathbb{R}^2$, $W_2(k) \in \mathbb{R}^1$, $k = 0, 1, 2\cdots$.

The integral term $W(k)$ given by (32) has to be intended as a stochastic Wiener integral, its covariance matrix is $E[W(k)W(k)^T] := Q_d(k) = \sigma_\eta^2(k)\bar{Q}(k)$, where:

$$\bar{Q}(k) = \begin{bmatrix} Q_{1,1}(k) & Q_{1,2}(k) \\ Q_{2,1}(k) & Q_{2,2}(k) \end{bmatrix} \tag{33}$$

$$\begin{aligned} Q_{1,1}(k) &= \begin{bmatrix} T + \nu^2(k-1)\frac{T^3}{3} sin^2\hat{\theta}(k,k) \\ -\nu^2(k-1)\frac{T^3}{3} cos\hat{\theta}(k,k) sin\hat{\theta}(k,k) \\ -\nu^2(k-1)\frac{T^3}{3} cos\hat{\theta}(k,k) sin\hat{\theta}(k,k) \\ T + \nu^2(k-1)\frac{T^3}{3} cos^2\hat{\theta}(k,k) \end{bmatrix}, \end{aligned} \tag{34}$$

$$Q_{1,2}(k) = \begin{bmatrix} -\nu(k-1)\frac{T^2}{2} sin\hat{\theta}(k,k) \\ \nu(k-1)\frac{T^2}{2} cos\hat{\theta}(k,k) \end{bmatrix}, \tag{35}$$

$$Q_{2,1}(k) = Q_{1,2}(k)^T, \quad Q_{2,2}(k) = T. \tag{36}$$

Denote by $Z(k)$ the measurement vector at time instant kT. Its dimension p_k is not constant, depending on the number of sensory measures that are actually used at each time. Vector $Z(k)$ is composed by two subvectors $Z_1(k) = [z_1(k),\ z_2(k)]^T$ and $Z_2(k) = [z_3(k),\ z_4(k),\ \cdots,\ z_{2+n_s}(k)]^T$.

The elements of $Z_1(k)$ are: $z_1(k) \equiv y_\nu(k)$, $z_2(k) \equiv \theta_g(k)$, where $y_\nu(k)$ is the measure related to the increments provided by the encoders through equations (9) and (13), $\theta_g(k)$ is the angular measure provided by the FOG. The elements of $Z_2(k)$ are: $z_{2+i}(k) = d_i^j(k) + n_{r,i}(k)$, $i = 1, 2, \ldots, n_s$, $1 \le j \le n_p$, with $d_i^j(k)$ given by (18). The environment map provides the information needed to detect which is the plane P^j in front of the laser.

The observation noise $V(k) = [\, n_\nu(k), n_\theta(k), n_{r,1}(k), \cdots, n_{r,n_s}(k)\,]$, is a white sequence $\sim N(0, R)$, where R has the structure: $R :=$ block diag $[R_1,\, R_2]$, with $R_1 :=$ diag$[\sigma_\nu^2,\, \sigma_\theta^2]$ and $R_2 :=$ diag$[\sigma_{r,1}^2,\, \sigma_{r,2}^2,\, \cdots,\, \sigma_{r,n_s}^2]$. The

diagonal form of R follows by the independence of the encoders, FOG and laser scanner measures.

As previously mentioned, the measure $z_2(\cdot)$ provided by the FOG is much more reliable than $z_1(\cdot)$ and $z_{2+i}(\cdot)$, $i = 1, 2, \cdots, n_s$, so that $\sigma_\theta^2 << \sigma_\nu^2$ and $\sigma_\theta^2 << \sigma_{r,i}^2$, $i = 1, 2, \cdots, n_s$. This gives rise to a nearly singular filtering problem, where singularity of R arises due to the very high accuracy of a measure. In this case a lower order non singular EKF can be derived assuming that the original R is actually singular [33]. In the present problem, assuming $\sigma_\theta^2 = 0$, the nullity of R is $m = 1$ and the original singular EKF of order $n = 3$ can be reduced to a non singular problem of order $n - m = 2$, considering the third component $\theta(\cdot)$ of the state vector $X(\cdot)$ coinciding with the known deterministic signal $z_2(\cdot) = \theta_g^r(\cdot)$. Under this assumption, only $X_1(\cdot)$ need be estimated as a function of $z_1(\cdot)$ and $Z_2(\cdot)$.

As the measures $z_1(\cdot)$ provided by the encoders are in terms of increments, it is convenient to define the following extended state $\bar{X}(k) := [X_1(k)^T,\, X_1(k-1)^T]^T$ in order to define a measure equation where the additive gaussian noise is white. The dynamic state-space equation for $\bar{X}(k)$ is directly derived from (22), taking into account that, by the assumption on $z_2(k)$, in all vectors and matrices defined in (25)–(36), the term $\hat{\theta}(k,k)$ must be replaced by $\theta_g^r(k)$.

The following equation is obtained

$$\bar{X}(k+1) = \bar{A}(k)\bar{X}(k) + \bar{L}(k)U(k) + \bar{B}(k)\theta_g^r(k) + \bar{D}(k) + \bar{W}(k), \quad (37)$$

where

$$\bar{A}(k) = \begin{bmatrix} I_2 & 0_{2,2} \\ I_2 & 0_{2,2} \end{bmatrix}, \quad (38)$$

$$\bar{L}(k) = \begin{bmatrix} L_1(k) \\ 0_{2,2} \end{bmatrix}, \quad \bar{B}(k) = \begin{bmatrix} A_{1,2_d}(k) \\ 0_{2,1} \end{bmatrix}, \quad (39)$$

$$\bar{D}(k) = \begin{bmatrix} D_1(k) \\ 0_{2,1} \end{bmatrix}, \quad \bar{W}(k) = \begin{bmatrix} W_1(k) \\ 0_{2,1} \end{bmatrix}, \quad (40)$$

$0_{i,j}$ being the $(i \times j)$ null matrix.

Equations (6), (7) and (13) and the way the state vector $\bar{X}(k)$ is defined imply that the $z_1(k) \equiv y_\nu(k)$ can be indifferently expressed as

$$z_1(k) = [\alpha(k)^{-1},\, 0,\, -\alpha(k)^{-1},\, 0]\bar{X}(k) + n_\nu(k), \quad (41)$$

or

$$z_1(k) = [0,\, \beta(k)^{-1},\, 0,\, -\beta(k)^{-1}]\bar{X}(k) + n_\nu(k), \quad (42)$$

where

$$\alpha(k) := \frac{sin\frac{\bar{\omega}(k)T}{2}}{\frac{\bar{\omega}(k)T}{2}} cos(\theta(k) + \frac{\bar{\omega}(k)T}{2})$$

$$\beta(k) := \frac{sin\frac{\bar{\omega}(k)T}{2}}{\frac{\bar{\omega}(k)T}{2}} sin(\theta(k) + \frac{\bar{\omega}(k)T}{2})$$

with $\bar{\omega}(k)T = \theta_g^r(k+1) - \theta_g^r(k)$ and $\theta(k) = \theta_g^r(k)$. The measure equations (41) and (42) can be combined to obtain a unique equation where $z_1(k)$ is expressed both as a function of $x(k+1) - x(k)$ and of $y(k+1) - y(k)$. As the amount of observation noise is the same, equations (41) and (42) are averaged, obtaining

$$z_1(k) = C_1(k)\bar{X}(k) + v_1(k), \quad (43)$$

where

$$C_1(k) = [\,\alpha(k)^{-1}/2,\ \beta(k)^{-1}/2,\ -\alpha(k)^{-1}/2,\ -\beta(k)^{-1}/2\,] \quad (44)$$

and $v_1(k) := n_\nu(k)$.

Vectors $Z_2(k)$ and $\bar{X}(k)$ are related by a non linear measure equation of the state and of the environment geometric parameter vector Π. The dimension $\overline{p}_k := p_k - 2$ of $Z_2(k)$ is not constant, depending on the number of laser scanner measures that are actually used at each time.

Linearization of the measure equation relating $Z_2(k)$ and $\bar{X}(k)$ about the current estimate of $\bar{X}(k)$ results in:

$$\bar{Z}_2(k) = C_2(k)\bar{X}(k) + V_2(k), \quad (45)$$

where $V_2(k) = [\,n_{r,1}(k),\, n_{r,2}(k),\, \cdots,\, n_{r,n_s}(k)\,]$, is a white noise sequence $\sim N(0, R_2)$ and

$$C_2(k) := [\,c_1(k)^T,\quad c_2(k)^T,\quad \cdots,\quad c_{\bar{p}_k}(k)^T\,]^T, \quad (46)$$

with

$$c_i(k) = \frac{P_\nu^j}{\cos\theta_d^j}\,[\,-cosP_n^j,\quad -sinP_n^j,\quad 0,\quad 0\,],$$
$$i = 1, 2, \ldots, \bar{p}_k, \quad \bar{p}_k \le n_s,\ 1 \le j \le n_p \quad (47)$$

and

$$\theta_d^j = P_n^j - \theta_g^r - \theta_r + \frac{\pi}{2}. \quad (48)$$

Equations (37), (43) and (45) represent the linearized, discretized state-space form to which the classical EKF algorithm has been applied.

IV. Laser Scanner Readings Selection

To reduce the probability of an inadequate interpretation of erroneous sensor data, a method is proposed to deal with the undesired interferences produced by the presence of unknown obstacles on the environment or by incertitude on the sensor readings. Notice that for the problem handled here both the above events are equally distributed. A simple and efficient way to perform this preliminary measure selection is to compare the actual sensor readings with their expected values. Measures are discharged if the difference exceeds a time-varying threshold. This is here done in the following way: at each step, for each measure $z_{2+i}(k)$ of the laser scanner, the residual $\gamma_i(k) = z_{2+i}(k) - \hat{d}_i^j$ represents the difference between the actual sensor measure $z_{2+i}(k)$ and its expected value $\hat{d}_i^j$, $i = 1, 2, \cdots, \bar{p}_k$, $j = 1, 2, \cdots, n_p$, which is computed by (18) on the basis of the current estimate of $\bar{X}(k)$. As $\gamma_i(k) \sim N(0, s_i(k))$, the current value $z_{2+i}(k)$ is accepted if $|\gamma_i(k)| \le 2\sqrt{s_i(k)}$ [34]. Namely, the variable threshold is chosen as two times the standard deviation of the innovation process.

V. Experimental results

The experimental tests have been performed on the TGR Explorer powered wheelchair [27] in an indoor environment. This vehicle has two driving wheels and a steering wheel. The odometric system is composed by two optical encoders connected to independent passive wheels aligned with the axes of the driving wheels. A sampling time of $0.4s$ has been used.

The odometric data are the incremental measures that at each sampling interval are provided by the encoders attached to the right and left passive wheels. The incremental optical encoders SICOD mod. F3-1200-824-BZ-K-CV-01 have been used to collect the odometric data. This encoders have $1200\,pulses/rev.$ and a resolution of $0.0013\,rad$. These measures are directly acquired by the low level controller of the mobile base. The gyroscopic measures on the absolute orientation have been acquired in a digital form by a serial port on the on-board computer. The fiber optic gyroscope HITACHI mod. HOFG-1 was used for measuring the angle θ of the mobile robot. The laser scanner measures have been acquired by the SICK LMS mod. 200 installed on the vehicle. The main characteristics of the FOG and LMS are reported in Tables I, II respectively.

TABLE I
Characteristics of the HITACHI gyroscope mod. HOFG - 1

Rotation Rate	-1.0472 to $+1.0472\,rad/s$
Angle Measurement Range	-6.2832 to $+6.2832\,rad$
Random Walk	$\leq 0.0018\,rad/\sqrt{h}$
Zero Drift (Rate Integration)	$\leq 0.0175\,rad/h$
Non-linearity of Scale Factor	within $\pm 1.0\%$
Time Constant	Typ. $0.02\,s$
Response Time	Typ. $0.02\,s$
Data Output Interval	Min. $0.01\,s$
Warm-up Time	Typ. $6.0\,s$

TABLE II
Characteristics of the SICK laser scanner mod. 200

Aperture Angle	$3.14\,rad$
Angular Resolution	$0.0175/\,0.0088/\,0.0044\,rad$
Response Time	$0.013/\,0.026/\,0.053\,s$
Resolution	$0.010\,m$
Systematic Error	$\pm 0.015\,m$
Statistic Error (1 Sigma)	$0.005\,m$
Laser Class	1
Max. Distance	$80\,m$
Transfer Rate	$9.6/\,19.2/\,38.4/\,500\,kBaud$

A characterization study of the Sick LMS 200 laser scanner has been performed as proposed in [35]. Different experiments have been carried out to analyze the effects of data transfer rate, drift, optical properties of the target surfaces and incidence angle of the laser beam. Based on empirical data a mathematical model of the scanner errors has been obtained. This model has been used as a calibration function to reduce measurement errors.

The TGR Explorer powered wheelchair with data acquisition system for FOG sensor, incremental encoders, sonar sensors and laser scanner is shown in Figure 5.

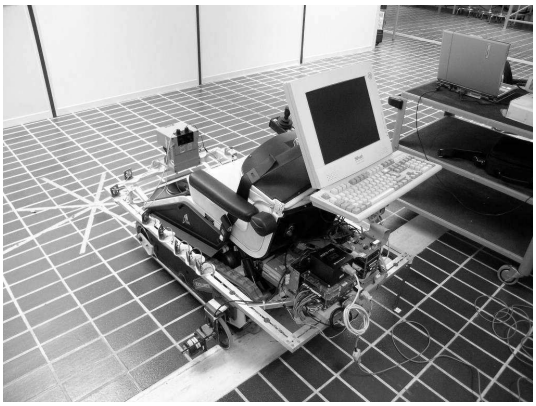

Fig. 5. TGR Explorer with data acquisition system for FOG sensor, incremental encoders, sonar sensors and laser scanner.

A significative reduction of the wrong readings produced by the presence of unknown obstacles has been realized by the selection of the laser scanner measures by the procedure described in Section IV.

The EKF has been implemented on the navigation module of the TGR Explorer powered wheelchair [27]. The navigation module developed for this vehicle interacts with the user in order to involve her/him in the guidance of the vehicle without limiting the functionality and the security of the system. The user sends commands to the navigation module through the user interface and the module translates the user commands in the low level command for the driving wheels. Two autonomy levels are developed to perform a simple filtering or for introducing some local corrections of the user commands on the basis of environment information acquired by the laser scanner (for more details see [25]). The navigation system is connected directly with the low level controller and with fiber optic gyroscope and laser scanner by analog and digital converters and serial ports RS232, respectively.

All the experiments have been performed making the mobile base track relatively long trajectories. Figures 6(a), 6(b) and 6(c) illustrate a sample of the obtained results. In the indoor environment of our Department a trajectory of $115m$ length, characterized by orientation changes has been imposed by the user interface. Figure 6 shows the trajectory of the vehicle estimated by the proposed algorithm and the considered indoor environment represented by a suitable set of planes orthogonal to the plane XY of the inertial system. The dots are the actually used laser scanner measures. The detected estimate errors in correspondence of the final vehicle configuration (the distance between the actual and the corresponding estimated configuration)

have been reported in Table III and are compared with the localization accuracy obtained by previously tested EKF integrating measures of different sensor equipments [2], [6]. The improvement introduced by EKF integrating Odometric, Inertial and Laser (OIL) measures with respect to EKF integrating Odometric, Inertial (OI) and Odometric, Inertial and Sonar (OIS) measures is confirmed by the comparison of the numerical values of the estimation errors, reported in the third column of Table III, with the values reported in the first and second column of Table III, respectively. This confirms the very high resolution and accuracy of the laser scanner measures. In spite of higher cost, compared to the sonar system, the localization procedure based on OIL measures does really seem to be an efficient tool to solve the SLAM problem.

TABLE III

Estimation errors (E) in correspondence of the final vehicle configuration (distance between the actual and the corresponding estimated configuration). OI=Odometric Inertial, OIS=Odometric Inertial Sonar, OIL=Odometric Inertial Laser

	$E(OI)$	$E(OIS)$	$E(OIL)$
x	$0.144\,m$	$0.095\,m$	$0.065\,m$
y	$0.795\,m$	$0.104\,m$	$0.072\,m$
θ	$0.043\,rad$	$0.025\,rad$	$0.013\,rad$

VI. Conclusions

In this note, an EKF is proposed as a tool for consistent fusion of informations acquired by the robot to reduce the uncertainties on the vehicle localization. The algorithm has been tested by a set of indoor experiments.

A novelty of the proposed EKF is that its formulation explicitly includes both the information carried by the model of the vehicle and the information carried by the observations. The algorithm operates in a state-space form were sensors and model uncertainties are intrinsically taken into account through the definition of a stochastic state-space model whose state vector contains the state variables of the wheelchair model. This introduces a very high degree of accuracy in the estimated vehicle trajectory and makes the estimator more robust with respect to possible uncertain physical parameters and/or not exactly known initial conditions. The appealing features of this approach are:

- the possibility of collecting all the available information and uncertainties of a different kind into a meaningful state-space representation,
- the recursive structure of the solution,
- the modest computational effort.

References

[1] A. Bemporad, M. Di Marco, and A. Tesi, "Sonar-based wall-following control of mobile robots," *Journal of dynamic systems, measurement, and control*, vol. 122, pp. 226–230, March 2000.

[2] A. Bonci, G. Ippoliti, L. Jetto, T. Leo, and S. Longhi, "Methods and algorithms for sensor data fusion aimed at improving the autonomy of a mobile robot," in *Advances in Control of Articulated and Mobile Robots*, B. Siciliano, A. De Luca , C. Melchiorri, and G. Casalino, Eds. Berlin, Heidelberg, Germany: STAR (Springer Tracts in Advanced Robotics), Springer-Verlag, 2004, vol. 10, pp. 191–222.

[3] J. Borenstein, H. R. Everett, L. Feng, and D. Wehe, "Mobile robot positioning: Sensors and techniques," *Journal of Robotic Systems*, vol. 14, no. 4, pp. 231–249, 1997.

[4] H. Durrant-White, "Sensor models and multisensor integration," *International Journal of Robotics Research*, vol. 7, no. 9, pp. 97–113, 1988.

[5] J. Gu, M. Meng, A. Cook, and P. Liu, "Sensor fusion in mobile robot: some perspectives," in *Proceedings of the 4th World Congress on Intelligent Control and Automation*, vol. 2, 2002, pp. 1194–1199.

[6] G. Ippoliti, L. Jetto, A. L. Manna, and S. Longhi, "Consistent on line estimation of environment features aimed at enhancing the efficiency of the localization procedure for a powered wheelchair," in *Proceedings of the Tenth International Symposium on Robotics with Applications - World Automation Congress (ISORA-WAC 2004)*, Seville, Spain, june 2004.

[7] F. Antoniali and G. Oriolo, "Robot localization in nonsmooth environments: experiments with a new filtering technique," in *Proceedings of the IEEE International Conference on Robotics and Automation (2001 ICRA)*, vol. 2, 2001, pp. 1591–1596.

[8] B. Barshan and H. Durrant-Whyte, "Inertial navigation systems for mobile robots," *IEEE Trans. Robot. Automat.*, vol. 11, pp. 328–342, Jun 1995.

[9] J. Castellanos, J. Neira, and J. Tards, "Multisensor fusion for simultaneous localization and map building," *IEEE Transactions on Robotics and Automation*, vol. 17, no. 6, pp. 908–914, 2001.

[10] I. Cox, "Blanche – an experiment in guidance and navigation of an autonomous robot vehicle," *IEEE Transactions on Robotics and Automation*, vol. 7, no. 2, pp. 193–204, April 1991.

[11] G. Dissanayake, S. Sukkarieh, E. Nebot, and H. Durrant-Whyte, "The aiding of a low-cost strapdown inertial measurement unit using vehicle model constraints for land vehicle applications," *IEEE Trans. on Robotics & Automation*, vol. 17, pp. 731–747, 2001.

[12] M. Dissanayake, P. Newman, S. Clark, H. Durrant-Whyte, and M. Csorba, "A solution to the simultaneous localization and map building (slam) problem," *IEEE Transactions on Robotics and Automation*, vol. 17, no. 3, pp. 229–241, June 2001.

[13] J. Guivant, F. Masson, and E. Nebot, "Simultaneous localization and map building using natural features and absolute information," *Robotics and Autonomous Systems*, pp. 79–90, 2002.

[14] K. Kobayashi, K. Cheok, K. Watanabe, and F. Munekata, "Accurate global positioning via fuzzy logic kalman filter-based sensor fusion technique," in *Proceedings of the 1995 IEEE IECON 21st International Conference on Industrial Electronics, Control, and Instrumentation*, vol. 2, Orlando, FL ,USA, Nov 1995, pp. 1136–1141.

[15] J. Leonard, H. Durrant-Whyte, and I. Cox, "Dynamic map building for autonomous mobile robot," in *Proceedings of the IEEE International Workshop on Intelligent Robots and Systems (IROS '90)*, vol. 1, Ibaraki Japan, July 1990, pp. 89 – 96.

[16] T. Levitt and D. Lawton, "Qualitative navigation fot mobile robots," *Artificial Intelligence Journal*, vol. 44, no. 3, pp. 305–360, 1990.

[17] I. Rekleitis, G. Dudek, and E. Milios, "Probabilistic cooperative localization and mapping in practice," in *Proceedings of the IEEE International Conference on Robotics and Automation (ICRA '03)*, vol. 2, Sept. 2003, pp. 1907 – 1912.

[18] S. Roumeliotis and G. Bekey, "Bayesian estimation and kalman filtering: a unified framework for mobile robot localization," in *Proceedings of the IEEE International Conference on Robotics and Automation (ICRA '00)*, vol. 3, San Francisco, CA, USA, apr 2000, pp. 2985–2992.

[19] S. Sukkarieh, E. Nebot, and H. Durrant-Whyte, "A high integrity imu/gps navigation loop for autonomous land vehicle

applications," *IEEE Trans. on Robotics & Automation*, vol. 15, pp. 572–578, 1999.
[20] S. Thrun, D. Fox, and W. Burgard, "A probabilistic approach to concurrent mapping and localization for mobile robots," in *Machine Learning Autonom. Robots*. Boston: Kluwer Academic Publisher, 1998, vol. 31, pp. 29–53.
[21] S. Williams, G. Dissanayake, and H. Durrant-Whyte, "An efficient approach to the simultaneous localization and mapping problem," in *Proceedings of the 2002 IEEE International Conference on Robotics and Automation*, Washington DC, USA, 2002, pp. 406–411.
[22] E. Zalama, G. Candela, J. Gòmez, and S. Thrun, "Concurrent mapping and localization for mobile robots with segmented local maps," in *Proceedings of the 2002 IEEE/RSJ Conference on Intelligent Robots and Systems*, Lausanne, Switzerland, 2002, pp. 546–551.
[23] G. Zunino and H. Christensen, "Simultaneous localization and mapping in domestic environments," in *Proceedings of the International Conference on Multisensor Fusion and Integration for Intelligent Systems (MFI 2001)*, 2001, pp. 67–72.
[24] G. Bourhis, O. Horn, O. Habert, and A. Pruski, "An autonomous vehicle for people with motor disabilities," *IEEE Robotics and Automation Magazine*, vol. 7, no. 1, pp. 20–28, 2001.
[25] S. Fioretti, T. Leo, and S. Longhi, "A navigation system for increasing the autonomy and the security of powered wheelchairs," *IEEE Transactions on rehabilitation engineering*, vol. 8, no. 4, pp. 490–498, 2000.
[26] E. Prassler, J. Scholz, and P. Fiorini, "A robotic wheelchair for crowded public environments," *IEEE Robotics and Automation Magazine*, vol. 7, no. 1, pp. 38–45, 2001.
[27] TGR-Bologna, *TGR Explorer*. Italy [Online]. Available: http://www.tgr.it., 2000.
[28] C. Wang, "Localization estimation and uncertainty analysis for mobile robots," in *Proceedings of the Int. Conf. on Robotics and Automation*, 1988, pp. 1230–1235.
[29] J. Borenstein and L. Feng, "Measurement and correction of systematic odometry errors in mobile robots," *IEEE Transaction on Robotics and Automation*, vol. 12, no. 6, pp. 869–880, dec 1996.
[30] H. Chung, L. Ojeda, and J. Borenstein, "Accurate mobile robot dead-reckoning with a precision-calibrated fiber-optic gyroscope," *IEEE Transactions on Robotics and Automation*, vol. 17, no. 1, pp. 80–84, 2001.
[31] K. Killian, "Pointing grade fiber optic gyroscope," in *Proc. of the IEEE Symposium on Position Location and Navigation*, Las Vegas, NV,USA, Apr 1994, pp. 165–169.
[32] R. Zhu, Y. Zhang, and Q. Bao, "A novel intelligent strategy for improving measurement precision of fog," *IEEE Transactions on Instrumentation and Measurement*, vol. 49, no. 6, pp. 1183–1188, Dec 2000.
[33] B. Anderson and J. Moore, *Optimal Filtering*. Prentice-Hall, Inc, Englewood Cliffs, 1979.
[34] L. Jetto, S. Longhi, and G. Venturini, "Development and experimental validation of an adaptive extended kalman filter for the localization of mobile robots," *IEEE Trans. on Robotics & Automation*, vol. 15, pp. 219–229, 1999.
[35] C. Ye and J. Borenstein, "Characterization of a 2d laser scanner for mobile robot obstacle negotiation," in *Proceedings of the IEEE International Conference on Robotics and Automation (ICRA '02)*, vol. 3, Washington, DC USA, May 2002, pp. 2512 – 2518.

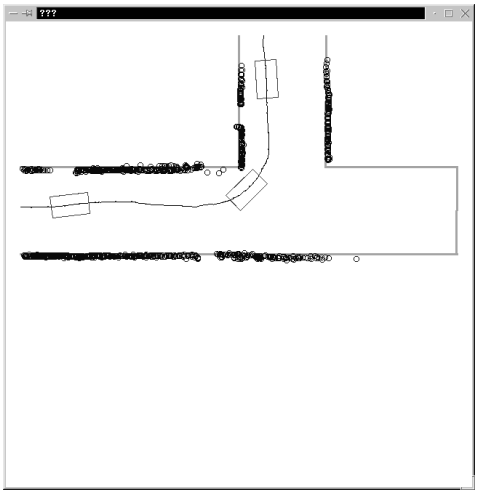

(a)

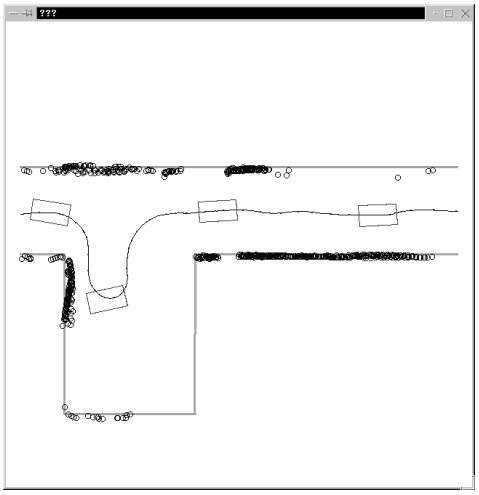

(b)

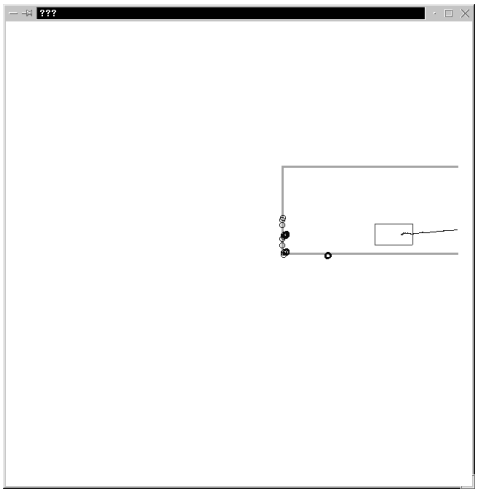

(c)

Fig. 6. Sample of the estimated trajectory. The dots are the actually used laser scanner measures.